Pergamon

PII: S0191-8141(96)00028-4

Journal of Structural Geology, Vol. 18, No. 8, pp. 1005 to 1016, 1996

0191-8141/96 $15.00+0.00

Magnetic fabric and microstructural evidence for a tectono-thermal overprint of the early Proterozoic Murray pluton, central Ontario, Canada

ULRICH RILLER, ALEXANDER R. CRUDEN and W. M. SCHWERDTNER

Department of Geology, University of Toronto, 22 Russell St., Toronto, Canada M5S 3B1

(*Received* 20 *June* 1995; *accepted in revised form* 20 *March* 1996)

Abstract—The 2.38 Ga old Murray granite pluton intruded the southern footwall of the Sudbury Igneous Complex and was subjected to repeated ductile deformation. Its NW and SE domains display differences in strain state, AMS signature and the nature and distribution of Fe-oxide minerals. The magnetic foliation is parallel to the visible foliation in the NW domain, but discordant to it in the SE domain. Microstructural data show that the magnetic fabric in the NW domain coincides with a foliation formed at high temperature, probably in response to thermal softening during the emplacement of the adjacent Sudbury Igneous Complex. This tectono-thermal overprint affected pre-existing shape fabrics and was facilitated by incipient melting of the granite near the intrusive contact with the Sudbury Igneous Complex. Rocks of the SE domain are only partially overprinted and two mineral subfabrics are preserved. Prolate susceptibility ellipsoids and clusters of maximum susceptibility directions at the intersections of the two planar fabrics suggest oblique superposition of strain increments. Increases in bulk magnetic susceptibility and magnetic anisotropy degree towards the intrusive contact with the Sudbury Igneous Complex can be explained by respective increases in the proportion of magnetite over ilmenite and strain intensity in the Murray pluton. Copyright © 1996 Elsevier Science Ltd

INTRODUCTION

Anisotropy of magnetic susceptibility (AMS) has been used in many structural studies as a tool for grain fabric analysis (Richter *et al.* 1993), as a strain indicator (Borradaile 1991, Housen *et al.* 1995) and for the quantitative analysis of magmatic fabrics in granitoid rocks (Bouchez *et al.* 1990, Archanjo *et al.* 1994, Cruden & Launeau 1994). Recent studies have shown AMS to be a potentially useful tool for the recognition of multiple deformation episodes in granitoids (Benn *et al.* 1993, Bouchez & Gleizes 1995). This paper reports the effects of post-crystallization deformation on the magnetic fabric and microstructure of the Murray pluton in central Ontario, Canada. Fine grain size and excellent exposure, allowing for a high density of structural field data, make this pluton a perfect target to study the relation between its magnetic and mineral shape fabrics (Riller *et al.* 1994).

The 2.38 Ga old Murray granite pluton is located in a narrow zone of lower amphibolite facies Huronian rocks at the northern margin of the Eastern Penokean Orogen (Fig. 1). This zone is part of the overturned southern footwall of the impact-related Sudbury Igneous Complex (SIC). The pluton was subjected to syn- to post-emplacement, early Proterozoic deformation, and later overprinted by solid-state strains and contact metamorphism during emplacement of the SIC at 1.85 Ga. The magnetic fabric analysis and micro-structural and petrographic observations of the Murray pluton reported here characterize the effects of a high-temperature metamorphic overprint by the SIC. The results provide new constraints on (1) the tectonometamorphic history of the Eastern Penokean Orogen (EPO), (2) the age and mechanisms of NW–SE shortening of the SIC and its wall rocks and (3) the origin of the norite of the SIC.

GEOLOGICAL SETTING

The Eastern Penokean Orogen

The EPO is an early Proterozoic fold-and-thrust belt that affected rocks of the Huronian Supergroup in the Southern Province and is located at the north shore of Lake Huron (Fig. 1). Two pulses of granitoid plutonism in the EPO have been dated, the Murray and Creighton pluton pulse at 2.3 Ga (Frarey *et al.* 1982, Krogh *et al.* 1984) and the Cutler and Grenville Front granite pulse at *ca* 1.7 Ga (Wetherill *et al.* 1960, Krogh & Davis 1969). Card (1978) recognized high-temperature metamorphic zones that are spatially associated with these plutons. Intrusion of the Murray and Creighton plutons and greenschist facies metamorphism have been attributed to the early Proterozoic Blezardian Orogeny in the Sudbury area (Stockwell 1982). Regional deformation in the EPO prior to emplacement of Nipissing Gabbro sills at 2.19 Ga (Corfu & Andrews 1986) may also be attributed to this orogeny (Card *et al.* 1972). Structures formed under amphibolite facies metamorphic conditions in the EPO are generally attributed to the Penokean orogeny (Card *et al.* 1972), which in the type area in the north-central U.S.A. occurred at 1.9–1.85 Ga (Van Schmus 1976).

Geology of the Sudbury area

Granites and greenstones of the Archean basement near Sudbury are overlain unconformably by amphibo-

lite facies mafic metavolcanics and intercalated metasedimentary rocks of the Elsie Mountain and Stobie Formations (Figs. 1 and 2). These are the lowermost units of the folded Huronian cover and are intruded by the Murray and Creighton plutons. The Huronian rocks are overturned and south-facing along the southern margin of the SIC and Archean basement. South of the Sudbury area, Huronian rocks are reworked and overthrust by Grenville Province gneisses and obscured by onlapping carbonates of the Paleozoic Michigan Basin.

The Sudbury Basin (Fig. 1) consists of a folded sedimentary core, the Whitewater Group, which is bound by concentric layers of norite, gabbro and granophyre of the SIC (Pye *et al.* 1984, Dressler *et al.* 1991). The SIC intrudes the Archean Levack Gneiss Complex in the north and Huronian metavolcanic rocks in the south. Emplacement of the SIC at 1.85 Ga (Krogh *et al.* 1984) is attributed either to a large volcanic explosion (Muir 1984) or to meteorite impact (Dietz 1964, Muir & Peredery 1984, Grieve *et al.* 1991). The crypto explosion created a variety of shock metamorphic structures, such as the Sudbury Breccia, and may have overturned the Huronian footwall rocks (see references cited).

STRUCTURE AND METAMORPHISM OF THE MURRAY PLUTON

The Murray pluton is a suboval (5×2 km) granite body in map view (Fig. 2). In the southeastern part of the pluton, a weakly developed mineral shape fabric defined by the preferred alignment of mafic clots, biotite and euhedral feldspar, appears to be of magmatic origin. In the NW part, adjacent to the SIC, interlayering of biotite and amphibole with felsic ribbons composed of recrystallized K-feldspar, plagioclase and elongate quartz indicates solid-state strain. Foliation intensities in the pluton are highest adjacent to the northwestern boundary and decrease towards the southeast, where the variation in strike of the foliation is greatest. Foliation trajectories, measured at 200 stations within, and 70 stations around the pluton, are shown in Fig. 2. Trajectories are not refracted where they cut obliquely across the pluton boundaries, indicating a low ductility contrast (Schwerdtner *et al.* 1985) between the granite and the metavolcanic wall rocks during imprint of this deformation. The strike of the foliation trajectories in the wall rocks is nearly constant and subparallel to northeast-striking lithologic contacts (Fig. 2). Within a *ca* 500 m wide contact metamorphic aureole of the SIC, Huronian metavolcanic rocks have a massive texture due to poikiloblastic growth of green hornblende. Preferred mineral orientations are also absent in the norite of the adjacent SIC.

Definition of structural domains

Two domains of contrasting foliation orientation and shape fabric geometry can be distinguished in the Murray pluton (Fig. 2). In the NW domain, the foliation strikes northeastward in an approximately 800 m wide zone which is subparallel to the contact with the unstrained norite of the SIC. Foliation trajectories in the SE domain strike east to east-southeast, except at a few localities which show northeast strike in the central part. Flat, glaciated exposures, and moderate to low finite strains in the Murray pluton, make it impossible to measure the orientation of the mineral lineation in the field.

To characterize the shape fabrics further, oriented specimens were cut parallel to foliation (S) and lineation (L) for determination of lineation orientation and fabric geometry (k-values, Flinn 1962). Visual appraisal of cut specimens (Table 1) revealed that linear fabrics ($L > S$) prevail in the SE domain and planar fabrics ($S > L$) dominate in the NW domain. The axial ratios of microgranitoid enclaves were also measured on suitable outcrop surfaces (Table 1). Where measurements could be made, enclave shapes correlate well with the visual estimates and are prolate ($k > 1$) in the SE domain, and close to plane strain ($k \approx 1$) in the NW domain. Lineations plunge moderately to steeply to the northwest (Table 1 and Fig. 2: orientation diagram). Before presenting results of the magnetic fabric analysis, we first outline the petrographic and microstructural characters of both domains.

SE domain. Metagranitic rocks of this domain are characterized by the extensive breakdown of plagioclase to euhedral epidote, (clino)-zoisite and albite. K-feldspars are present as perthitic microclines. Quartz is recrystallized into equigranular aggregates displaying undulatory as well as straight extinction and polygonal grain boundaries. Large flakes of brown biotite of probably primary magmatic origin are often kinked and transformed to finer grained green–brown biotite, chlorite and muscovite. Approaching the NW domain, brown biotite is progressively replaced by blue–green actinolitic hornblende. Ilmenite and sphene are associated with the secondary biotite and blue–green hornblende. Greenschist facies metamorphic conditions are indicated by the transformation of brown (Ti-rich) biotite into green (Ti-poor) biotite, muscovite, ilmenite and sphene (Kerrich *et al.* 1980, Vernon *et al.* 1983) and by the metamorphic assemblage of albite + epidote ± zoisite + actinolite + chlorite + quartz. The preferred orientation of metamorphic biotite and hornblende in the SE domain (see below) suggests that deformation was synchronous with this metamorphism.

NW domain. The NW domain is characterized by major changes in (1) the textures of felsic minerals, (2) the oxide mineralogy, (3) the metamorphism, and (4) the fabric intensity as compared to the SE domain. Quartz shows a large grain size and is present both as recovered, strain-free polygonized aggregates with dihedral angles of 120° at triple junction boundaries, and as dynamically recrystallized aggregates with sutured grain boundaries and core–mantle structure. Recrystallized plagioclase grains are sometimes replaced by epidote and zoisite.

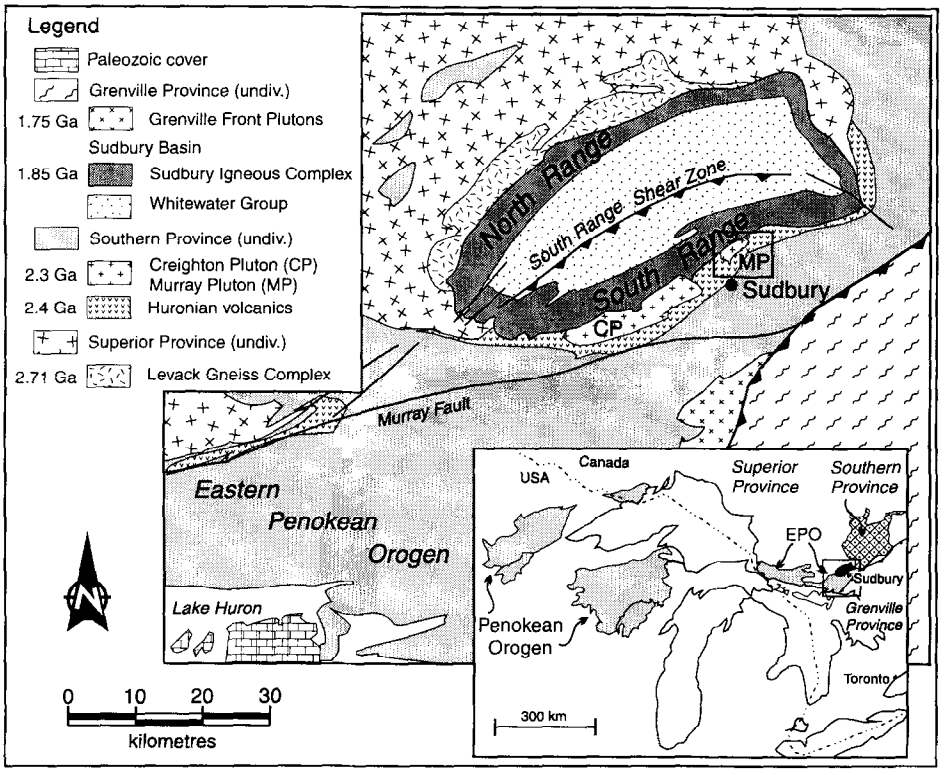

Fig. 1. Simplified geological map showing major structural units in the Sudbury area of the Eastern Penokean Orogen. Box indicates location of Fig. 2. Inset shows the extent of the early Proterozoic Penokean Orogen and Southern Province in the Great Lakes area (after Thurston 1991). EPO — Eastern Penokean Orogen on the north shore of Lake Huron.

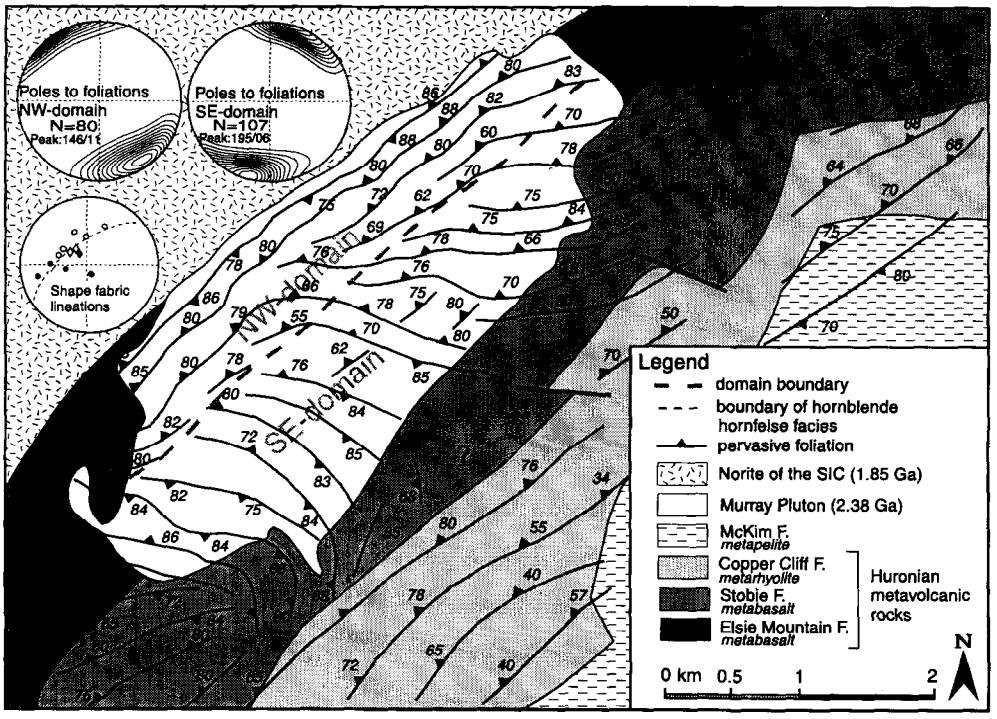

Fig. 2. Structure of the Murray pluton and its wall rocks. Solid lines are foliation trajectories with dip directions (barbs) and dip values. Foliation trajectories are discordant to, and non-refracted at, the southeastern boundary of the pluton. Note the absence of directional fabrics in both Huronian rocks and norite adjacent to the contact of the norite of the SIC. Lower hemisphere equal-area projections show foliations (contour interval is 2σ) measured in the field and linear fabric data from Table 1 (circles: shape fabric lineations, lozenges: enclave lineations, solid symbols: NW domain, open symbols: SE domain).

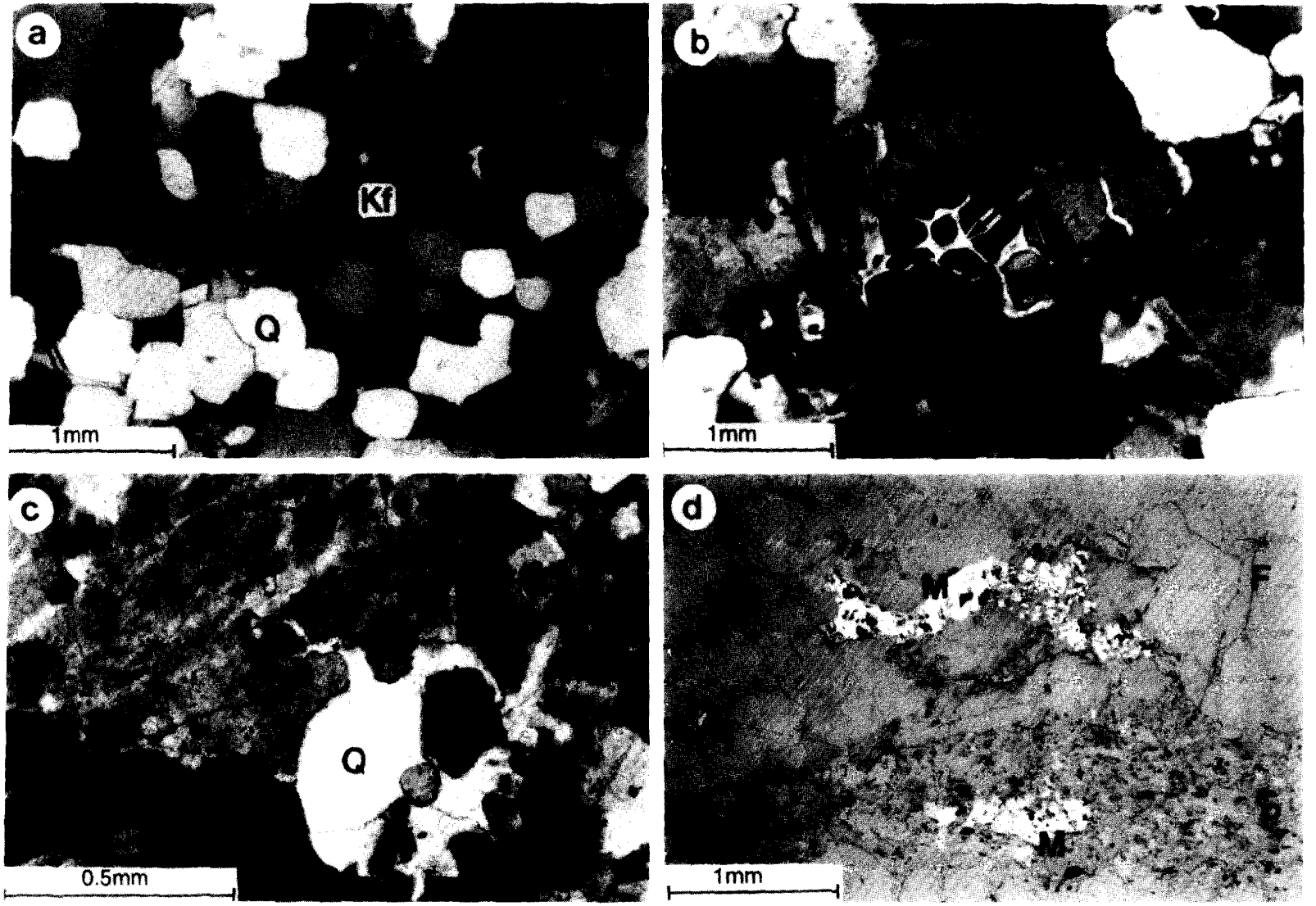

Fig. 3. Microstructure of metagranitic rocks from the NW domain of the Murray pluton. (a) Anhedral, recrystallized K-feldspar (Kf) is enveloped by recovered, strain-free quartz (Q). Note the characteristic dihedral angles of 120° at triple junctions in quartz (sample 9403, cross polars). (b) Quartz film (arrow) around corroded K-feldspar (Kf) indicates incipient melting in the granite (sample 9403, cross polars). (c) Unstrained quartz (arrow) is relocated in a fracture of recrystallized K-feldspar (sample 9403, cross polars). (d) Alignment of magnetite grains (M) with the foliation delineated by phyllosilicates (P) and felsic minerals (F) (sample 9328, reflected light).

Table 1. Orientation and geometry of shape fabrics in the Murray pluton

Shape fabrics					Enclave shapes							
Station	Domain	S	L	Geometry	Station	Domain	N	S	L	R_{AB}	R_{BC}	k
9311	SE	336/50	024/38	$L > S$	1075b	NW	35	330/80	320/75	3.17	2.37	1.6
9316	SE	342/66	285/52	$L > S$	1078	SE	18	325/78	315/70	3.03	1.48	4.2
9328	NW	266/64	264/62	$S > L$	1080	SE	13	010/70	305/65	3.00	1.50	4.0
9329	SE	335/62	300/54	$L > S$								
9330	SE	—	336/47	$L > S$								
9331	SE	—	355/57	$L > S$								
9401	NW	180/80	166/76	$S > L$								
9403	NW	328/72	255/22	$S > L$								
9404	NW	310/55	270/47	$S > L$								

N: number of measurements.
S: foliation (dip direction/dip).
L: Lineation (azimuth/plunge).
R_{AB} and R_{BC}: principal shape fabric ratios of the AB and BC planes of the shape fabric ellipsoid ($A \geq B \geq C$).
$k = (R_{AB}-1)/(R_{BC}-1)$.
See Fig. 4 for station location.

Small interstitial plagioclase crystals are zoned. K-feldspar is recrystallized into subgrains of perthitic microcline. Recovered quartz aggregates are found near irregular, recrystallized feldspar that does not show grain growth or recovery (Fig. 3a). A peculiar texture in the NW domain is the presence of K-feldspars showing corroded boundaries that are enveloped by thin films of largely unstrained quartz (Fig. 3b). Quartz is also located within fractures and around subgrains of K-feldspar whereby its shape is strongly controlled by the boundaries of the K-feldspar host grains (Fig. 3c). These quartz films are interpreted as intergranular silicate melt related to incipient melting of the granite (Van der Molen & Paterson 1979, Hibbard 1987). Brown biotite is almost entirely recrystallized to either small aligned grains or transformed to blue–green hornblende. Magnetite is the dominant Fe-oxide mineral and is associated with abundant epidote and sphene. It is aligned parallel to phyllosilicate- and hornblende-rich foliae, quartz ribbons and elongate feldspar (Fig. 3d) and is intergrown with ilmenite close to the domain boundary.

The parallelism of metamorphic biotite and hornblende with ribbons of recrystallized quartz and feldspar shows that growth of these minerals was coeval with fabric development. Recrystallization of feldspar generally requires temperatures above 450°C (Voll 1980, Tullis 1983) in agreement with the formation of biotite and hornblende in metagranitic rocks (Winkler 1979, p. 283). Incipient-melting features displayed by thin quartz seams around K-feldspars indicate that the melting temperature was transiently reached in a strain-free environment. However, quartz ribbons, straight subgrain boundaries and undulatory extinction in quartz suggest that some strain occurred as the temperature decreased. Deformation of the granite in the NW domain must therefore have occurred close to its solidus temperature. The presence of strain-free but comparatively large quartz crystals with respect to the size of recrystallized K-feldspar subgrains in some samples can be explained by different rates of annealing at high temperatures (Vernon *et al.* 1983).

These observations show that mineral fabrics (orientation, intensity and geometry) between the two domains of the Murray pluton are different. A strong metamorphic gradient across the pluton is indicated by greenschist facies metamorphic mineral assemblages in the SE domain versus textures formed close to the solidus temperature of granite near the contact with the SIC. However, the fabric data are qualitative and, because only few mineral lineations have been determined, are insufficient for the discrimination between possible kinematic hypotheses explaining the origin of domains and the observed curvature of the foliation in the Murray pluton. These hypotheses include (1) shearing parallel to the NW contact with the SIC and (2) oblique superposition of strains. In an attempt to differentiate between these models, quantitative information on fabrics at the grain scale and fabric intensity variations are examined using AMS as a tool.

MAGNETIC FABRIC STUDY

The analysis of magnetic susceptibility anisotropy (AMS) is now used routinely in geology (Rochette *et al.* 1992, Tarling & Hrouda 1993 and references therein). AMS is a symmetric tensor of second rank (Nye 1957) which relates the induced magnetization vector in a rock to the applied magnetic field vector. The tensor is conveniently represented by a triaxial magnitude ellipsoid, whose principal axes are the maximum, intermediate and minimum susceptibilities ($k_{max} \geq k_{int} \geq k_{min}$), measured in dimensionless SI units per unit volume. A magnetic fabric is characterized by the magnetic lineation (k_{max}) and the magnetic foliation (k_{max}/k_{int} plane). Two logarithmic parameters (Jelinek 1981) are recommended for the description of bulk susceptibility ellipsoid properties. The degree of anisotropy or AMS intensity is given

by $P' = \exp[2(a_1^2 + a_2^2 + a_3^2)]^{1/2}$, where $a_1 = \ln(k_{max}/K)$, etc. and $K = (k_{max} + k_{int} + k_{min})/3$, incorporating the three principal susceptibilities as well as their mean. The shape is given by $T = [2(\ln k_{int} - \ln k_{min})/(\ln k_{max} - \ln k_{min})] - 1$. Positive values ($0 < T \leq 1$) correspond to oblate ellipsoids while negative ones ($-1 \leq T < 0$) correspond to prolate ellipsoids.

At low field strength and room temperature, the bulk magnetic susceptibility, K, depends on the contributions of dia-, para- and ferrimagnetic minerals. The anisotropy of magnetic susceptibility is related to crystal lattice orientations of dia- and paramagnetic minerals and to shape-preferred orientations of ferrimagnetic minerals. Hargraves *et al.* (1991) also suggest that an anisotropic distribution of magnetite grains can cause AMS in some rocks. Susceptibilities of the rock-forming diamagnetic (e.g. quartz, calcite) and paramagnetic minerals (e.g. phyllosilicates, amphiboles) are in the order of 10^{-5}, and 10^{-4} to 10^{-3} SI/vol respectively. These are one to two orders of magnitude lower than the susceptibilities of the generally accessory ferrimagnetic minerals (e.g. magnetite), typically about 10^{-2} SI/vol (Tarling & Hrouda 1993). Therefore, correlations between the susceptibility ellipsoid and the petrofabric may not always be straightforward and complementary petrologic and/or rock magnetic analyses are often required to evaluate the geological significance of AMS fabrics (Rochette *et al.* 1992). Nonetheless, a good correlation between magnetic and crystalline fabrics in weakly strained granitoids has been repeatedly documented in previous studies (Benn *et al.* 1993, Cruden & Launeau 1994, Archanjo *et al.* 1995).

Magnetic fabric data

Three sample traverses with a total of 30 sample sites cross the Murray pluton perpendicular to the contact with the SIC (Fig. 4 and Table 2). Three to six 2.2 cm long and 2.54 cm diameter rock cylinders per site were prepared in the laboratory, resulting in a total of 138 specimens. The AMS of the specimens was measured at low magnetic field using an SI-2 induction coil instrument. The accuracy of susceptibility measurements is estimated to be >98% for samples with $K \geq 4 \times 10^{-4}$ SI. AMS data from each site were averaged using the tensor averaging method of Hext (1963) and Jelinek (1978) with the program *APLOT9* of Lienert (1991). AMS parameters describing ellipsoid shape T and intensity P' were calculated using the program *FABRIC* of G. Borradaile (Lakehead University). The quality of AMS orientations are measured by α_{95} confidence angles about the mean principal susceptibility axes for each site (Table 2).

Results

The site mean orientations of magnetic foliations in the Murray pluton are displayed by trajectories in Fig. 5(a). These trajectories trend NE–SW parallel to the pluton's long axis and to the contact with the SIC, except in the southeast where they strike E–W. The magnetic foliation dips predominantly towards the northwest and is steeply

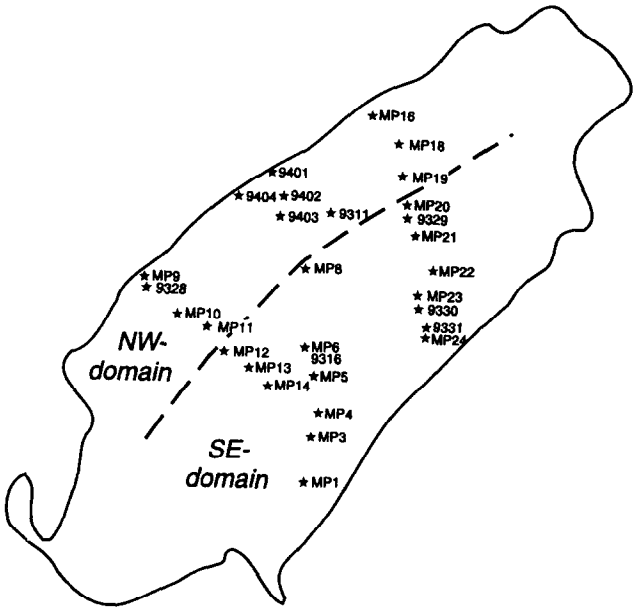

Fig. 4. Sample location map for AMS and shape fabric determination, stippled line delineates boundary between structural domains of the Murray pluton.

inclined near the borders and moderately in the central portion of the pluton. The most remarkable feature is that the magnetic foliation is close in orientation to the mineral foliation mapped in the NW domain, but is strongly oblique to mineral foliations observed in the SE domain (Fig. 5a). Magnetic lineations plunge to the west and northwest, and are steep along the northwest border, and moderate to shallow in the center of the pluton (Fig. 5b).

Variations between the NW and SE domains in scalar parameters of the magnetic fabric are shown in Fig. 6. Oblate AMS ellipsoids (Fig. 6a) and higher anisotropy degrees occur in the NW domain whereas neutral to prolate fabrics with lower anisotropy degrees characterize the SE domain, in accord with the observed mineral shape fabrics (Table 1). Most bulk susceptibilities in the SE domain cluster around 10^{-4} SI, except some samples showing a steady increase to *ca* 10^{-2} SI, along with an increase in anisotropy degree from $P' = 1.02$ to $P' = 1.13$ (Fig. 6b). Low K-values ($< 10^{-3}$ SI) indicate a predominantly paramagnetic source for the magnetic susceptibility (Rochette 1987), in accordance with ilmenite, phyllosilicates and hornblende observed in thin section. The replacement of ilmenite by magnetite in the NW domain explains the increase in K to values typical of ferrimagnetic susceptibilities $K \approx 10^{-2}$ SI. The increase in anisotropy degree P' with increasing susceptibility displayed by samples from the SE domain may be interpreted in terms of proportional increase of Fe-oxide minerals (Borradaile 1987). The NW domain is characterized by uniformly high bulk susceptibility up to $K = 10^{-2}$ SI, and anisotropy degree of up to $P' = 1.46$ (Fig. 6b). Such high K-values are indicative of a ferrimagnetic origin for the magnetic susceptibility in agreement with abundant magnetite grains identified in thin section. The large variation of P' at constant K-

Table 2. AMS site mean values of the Murray pluton

Site	N	Domain	K	Maximum susceptibility axes			Intermediate susceptibility axes			Minimum susceptibility axes					
				D/I	α_{95}	k_{max}	D/I	α_{95}	k_{int}	D/I	α_{95}	k_{min}	MF	P'	T
9401	5	NW	2.41E−2±2.83E−3	235/85	10:06	2.76E−2	075/02	12:05	2.38E−2	345/02	12:10	2.13E−2	165/88	1.30	−0.12
9402	6	NW	2.24E−2±1.55E−3	213/71	17:04	2.37E−2	058/17	17:06	2.28E−2	326/07	07:01	2.08E−2	146/83	1.14	0.40
9403	4	NW	2.43E−2±1.73E−3	257/27	14:03	2.59E−2	008/35	14:05	2.50E−2	139/43	05:03	2.22E−2	319/47	1.18	0.57
9404	5	NW	1.14E−2±1.40E−3	241/66	06:01	1.15E−2	042/23	07:05	1.17E−2	136/07	07:03	1.00E−2	316/83	1.26	0.39
9331	5	SE	1.09E−4±3.16E−4	026/59	58:18	1.11E−4	186/29	59:43	1.09E−4	281/09	49:29	1.06E−4	101/81	1.04	0.13
9330	5	SE	2.13E−4±4.14E−5	327/40	18:06	2.18E−4	155/50	79:10	2.11E−4	070/04	79:16	2.11E−4	240/86	1.04	−0.94
9329	6	SE	1.29E−4±4.30E−6	291/63	39:15	1.30E−4	052/15	39:19	1.29E−4	148/22	24:15	1.27E−4	329/78	1.03	0.18
9328	6	NW	1.39E−2±2.26E−3	270/50	31:12	1.55E−2	012/10	13:05	1.45E−2	110/38	31:03	1.21E−2	290/52	1.30	0.45
9316	6	SE	1.98E−4±8.80E−6	304/48	23:13	2.00E−4	081/33	38:21	1.97E−4	186/23	39:10	1.96E−4	006/77	1.02	−0.45
9311	6	NW	2.38E−4±8.30E−6	019/20	47:10	2.40E−4	288/05	47:24	2.39E−4	185/69	25:10	2.34E−4	005/21	1.03	0.54
MP01	5	SE	1.53E−2±2.20E−3	283/41	22:03	1.61E−2	099/49	29:07	1.53E−2	192/02	30:20	1.46E−2	012/88	1.11	−0.08
MP03	3	SE	1.14E−2±1.48E−3	288/50	63:11	1.21E−2	098/39	84:54	1.12E−2	192/05	84:33	1.09E−2	012/85	1.12	−0.60
MP04	3	SE	6.68E−3±6.16E−4	277/43	50:15	7.06E−3	035/27	54:30	6.65E−3	146/35	48:02	6.34E−3	326/55	1.11	−0.12
MP05	3	SE	1.49E−3±1.85E−4	297/46	60:46	1.51E−3	038/11	75:36	1.49E−3	138/42	75:35	1.47E−3	318/48	1.03	0.07
MP06	3	SE	1.95E−4±5.00E−6	253/44	81:40	1.98E−4	068/46	81:53	1.95E−4	161/03	65:16	1.91E−4	341/87	1.03	0.12
MP08	3	SE	7.08E−4±2.39E−4	287/19	61:33	7.34E−4	029/30	73:31	7.06E−4	350/36	72:43	6.86E−4	350/36	1.07	−0.13
MP09	3	NW	1.41E−2±1.86E−3	253/67	40:05	1.61E−2	357/06	50:15	1.45E−2	269/67	46:13	1.20E−2	269/67	1.35	0.26
MP10	3	NW	2.60E−3±1.23E−4	284/36	60:16	2.67E−3	034/25	67:07	2.62E−3	150/44	19:15	2.50E−3	330/46	1.07	0.46
MP11	3	NW	3.18E−3±2.43E−4	060/25	75:42	3.28E−3	278/59	75:71	3.23E−3	158/17	73:54	3.04E−3	337/73	1.08	0.63
MP12	4	SE	8.41E−3±1.48E−3	259/41	37:22	8.74E−3	013/26	38:27	8.38E−3	125/38	38:25	8.13E−3	305/52	1.08	−0.14
MP13	4	SE	1.60E−3±1.82E−4	290/26	43:15	1.66E−3	029/17	41:04	1.62E−3	148/58	25:07	1.54E−3	328/32	1.08	0.31
MP14	4	SE	2.03E−4±1.55E−5	263/22	71:33	2.04E−4	017/46	70:11	2.03E−4	156/37	50:26	2.01E−4	336/54	1.01	0.14
MP16	4	NW	2.20E−2±4.45E−3	341/70	11:06	2.55E−2	241/04	10:10	2.35E−2	149/20	12:03	1.78E−2	330/70	1.46	0.53
MP18	4	NW	1.33E−4±1.65E−5	276/71	38:13	1.37E−4	073/17	41:18	1.33E−4	165/07	32:11	1.30E−4	345/83	1.05	−0.02
MP19	3	NW	1.04E−2±1.53E−3	294/55	51:14	1.21E−2	045/12	53:04	1.04E−2	142/32	29:15	8.88E−3	322/58	1.37	0.02
MP20	3	SE	1.22E−4±8.00E−6	291/61	83:61	1.25E−4	025/02	83:23	1.22E−4	116/29	65:53	1.19E−4	296/61	1.04	−0.05
MP21	4	SE	1.30E−4±2.16E−5	323/41	65:14	1.32E−4	068/17	66:49	1.29E−4	175/44	56:04	1.28E−4	355/46	1.03	−0.22
MP22	4	SE	1.84E−4±2.24E−5	296/46	37:12	1.86E−4	074/36	33:18	1.84E−4	181/22	38:19	1.82E−4	001/68	1.02	−0.04
MP23	3	SE	1.12E−4±4.70E−6	286/55	76:27	1.15E−4	066/28	83:73	1.11E−4	167/18	83:13	1.09E−4	346/71	1.05	−0.14
MP24	7	SE	1.04E−4±1.08E−5	337/76	44:15	1.05E−4	101/08	41:29	1.04E−4	193/12	38:24	1.03E−4	013/78	1.03	−0.07

N: number of measurements per site. K: bulk susceptibility.
k: magnitude of the susceptibility axes in SI units. D and I: declination and inclination respectively.
α_{95}: denotes the maximum:minimum angles of the 95% confidence ellipse about the mean principal axis. MF is the magnetic foliation orientation (k_{max}/k_{int} plane). For explanation of P' and T parameters see text.

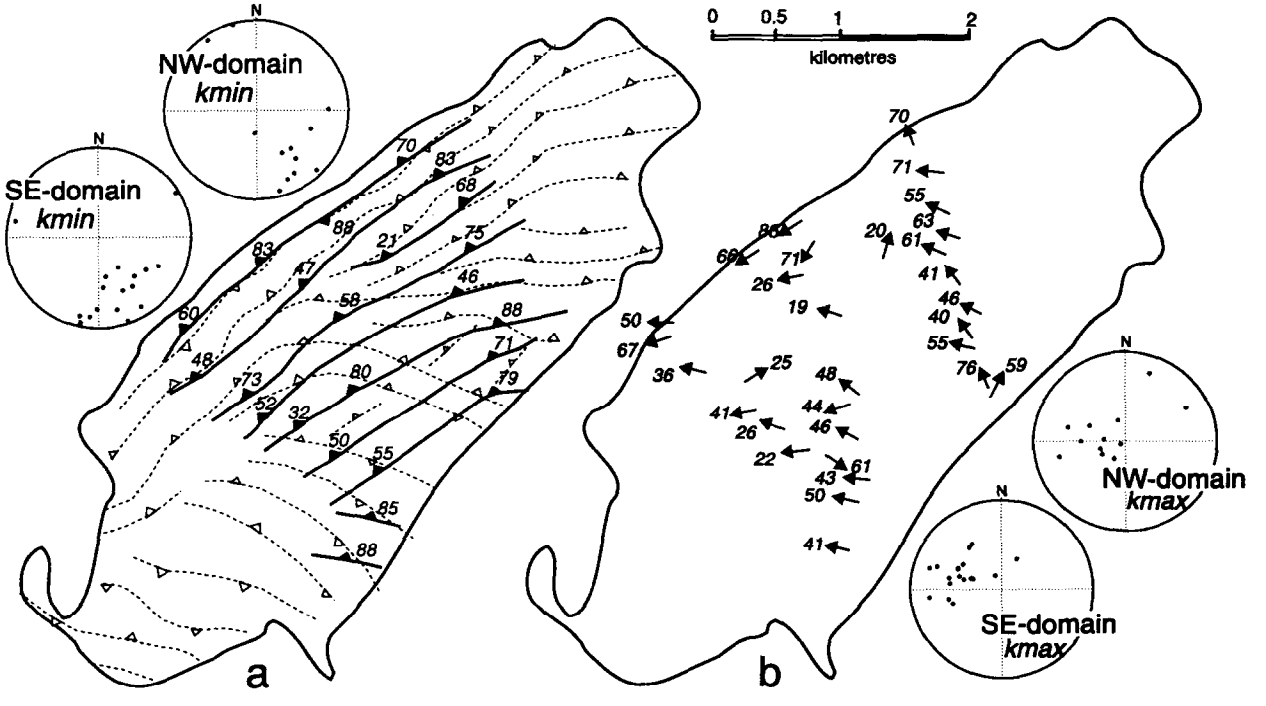

Fig. 5. (a) Trajectories of magnetic foliations (solid lines with barbs and dip values) and mineral foliations measured in the field (stippled lines with open barbs). Magnetic foliations are concordant to mineral foliations of the NW domain but highly discordant to those of the SE domain. Poles to magnetic foliations (k_{min}) are displayed on lower hemisphere equal-area projections. (b) Orientation of magnetic lineations (k_{max}).

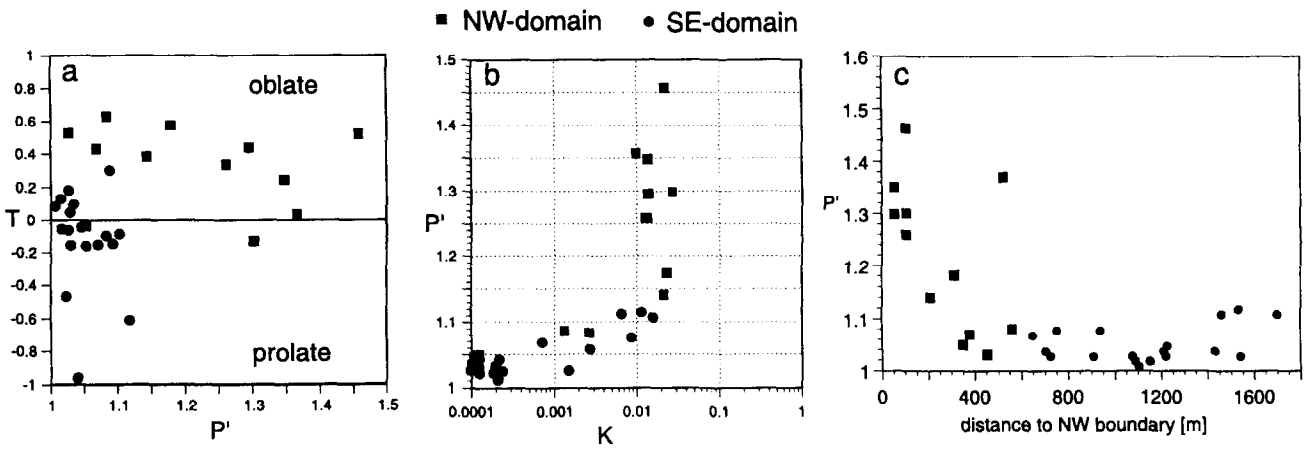

Fig. 6. Site-mean magnetic fabrics in the Murray pluton. For definition of fabric parameters refer to text. (a) Ellipsoid shape T versus anisotropy degree P'. Oblate geometry, and higher intensity dominate in the NW domain, whereas prolate susceptibility ellipsoids with lower intensities characterize the SE domain. (b) K vs. P'. The increase in K from 10^{-4} to 10^{-2} and the increase in P' in the SE domain are interpreted to be due to a variation in Fe-oxide mineralogy. Extreme variations of P' at rather constant K in the NW domain are related to variations in fabric intensity. (c) P' vs. distance from the contact with the SIC. A strong gradient of anisotropy degree in the NW domain, and constant values in the SE domain are observed.

values is unlikely to be related to a variation in mineralogy but reflects rather, a variation in the degree of preferred orientation and ellipticity of magnetite grains (i.e. fabric intensity) and/or magnetic interaction of magnetite due to clustering of grains (Hargraves *et al.* 1991, Stephenson 1994, Archanjo *et al.* 1995). The association of anisotropic magnetites with, and their alignment parallel to foliae defined by metamorphic hornblende and biotite (Fig. 3d) suggests that magnetite is metamorphic in origin. The increase in metamorphic grade toward the northwest may have resulted in a concentration of magnetite mimicking the shape fabric of mafic minerals in the NW domain. The steady increase in P' towards the contact with the SIC (Fig. 6c) is compatible with the observed increase in syn-contact metamorphic fabric intensity. However, very high P'-values (> 1.3) may also be indicative of magnetic fabric enhancement due to the magnetic interaction of magnetite grains (Archanjo *et al.* 1995, Grégoire *et al.* 1996).

Significance of the magnetic fabrics

The principal susceptibility directions at selected sites are compared to mineral fabrics measured in the field (Fig. 7). Principal directions at sites in the NW domain are tightly clustered and there is a close correlation between magnetic and mineral foliations (Fig. 7b). Similarly, k_{max} directions are within 10° of the mineral lineation (compare Tables 1 and 2). By contrast, the magnetic directions and observed petrofabrics are strongly discordant in the SE domain (Fig. 7a). k_{max} directions are well clustered, whereas k_{int} and k_{min} tend to spread out on great circles, as is expected given the prolate shapes of AMS ellipsoids in this domain (Fig. 6a). Interestingly, magnetic lineations (k_{max}) are located close to intersection of the magnetic and mesoscopic mineral foliations at each site. These relationships are now investigated further by microstructural examination and petrofabric measurements.

Thin sections oriented perpendicular to k_{max} of two samples from the SE domain and two samples from the NW domain reveal mineral subfabrics displayed as rose diagrams with respect to k_{int} and k_{min} in Fig. 8. The left-hand diagrams of Fig. 8(a)–(c) represent the preferred orientation of the large brown biotite flakes and the right-hand ones the preferred orientation of recrystallized green biotite and/or metamorphic hornblende. In Fig. 8(d), the alignment of hornblende and magnetite is shown. In samples 9311, 9316 and 9329 (Fig. 8a–c) the long axes of metamorphic biotite and hornblende are clustered around k_{int}, in contrast to the mean directions of brown biotite, which are less well constrained, and show an up to 80° obliquity to the k_{int} and the metamorphic mineral fabric. Except near the domain boundary (specimen 9311, Fig. 8c) only a single fabric is visible in thin sections from the NW domain. Here, magnetite shows a strong shape-preferred orientation subparallel to metamorphic hornblende (specimen 9328, Fig. 8d). The low scatter of long axis directions of both minerals in this plane is in accord with the planar character of the mineral shape fabric and its strong correlation with the magnetic fabric in the NW domain.

Susceptibility values and the above petrographic observations indicate that AMS in the Murray pluton is controlled by the alignment of magnetite, ilmenite, hornblende and biotite. In the NW domain, the magnitudes of both the magnetic susceptibility and its anisotropy (Fig. 6b) demonstrate that magnetite is the dominant carrier of the magnetic fabric. Its parallelism with metamorphic hornblende and biotite accounts for the observed coaxiality of the AMS and the metamorphic petrofabric in this domain. By contrast, low magnetic susceptibilities dominate the SE domain (Fig. 6b) and exclude magnetite as the major source for AMS. Of the two subfabrics present in the SE domain, the one defined by the minerals of highest magnetic susceptibility and/or highest modal abundance is most likely to be delineated by the AMS. Electron microprobe determination of

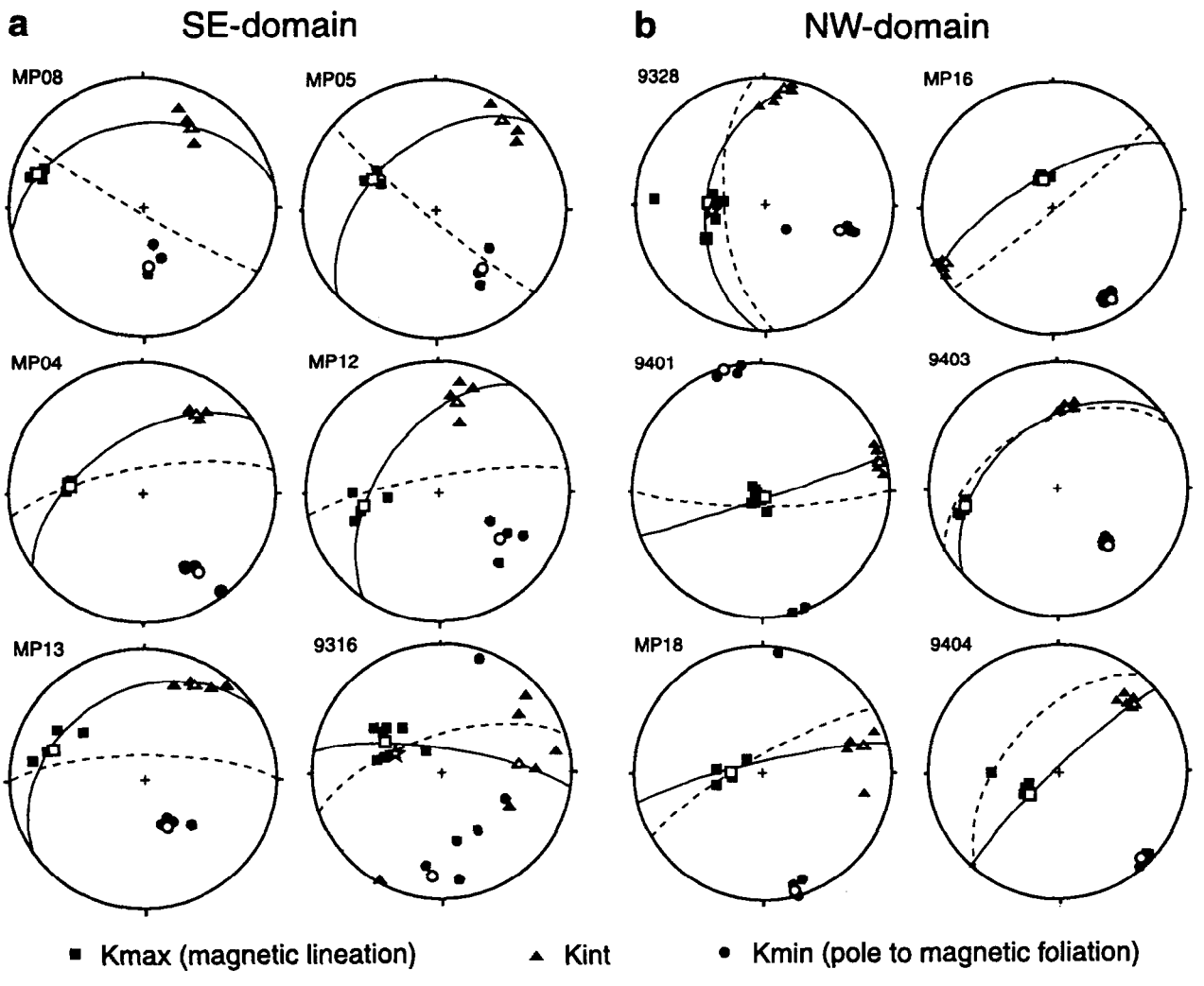

Fig. 7. Orientation of principal susceptibility axes at selected sites in the SE domain (a) and NW domain (b). Solid great circles are the site mean of magnetic foliations (k_{max}/k_{int} planes). Stippled great circles are foliations measured in outcrop. Stars at locations 9328 and 9316 indicate the long axis of mineral fabric ellipsoids (see Table 2). Note the close correlation of magnetic lineations (k_{max}) with the intersections of great circles in diagrams from the SE domain.

compositions of metamorphic hornblendes and brown biotites shows that they have similar Fe contents. Hence, the susceptibility of these minerals is not likely to be significantly different (Tarling & Hrouda 1993 p. 49). However, the modal abundance of hornblende is generally higher than that of biotite and increases greatly towards the northwest, suggesting that AMS in the SE domain is related to the lattice-preferred orientation of metamorphic hornblende rather than that of biotite. The stubby shape and small size of hornblende crystals may explain why the NE-trending metamorphic hornblende + ilmenite ± green biotite fabric in the SE domain remained largely undetected in the field, in contrast to the E- to ESE-trending biotite fabric (Fig. 2).

Parallelism of magnetic lineations with the lines of intersecting planar fabrics has been often observed in cleaved metasediments (Borradaile & Tarling 1981, Rochette & Vialon 1984, Housen *et al.* 1993). Housen *et al.* (1993) found that the orientation of k_{int} and k_{min} are strongly controlled by the subfabric containing the higher magnetic susceptibility minerals, which is consistent with the lattice-preferred orientation of metamorphic hornblende ± green biotite in the SE domain of the Murray pluton. The origin of k_{max} in this domain seems to be controlled by the intersection of the metamorphic fabric with the primary biotite fabric (Fig. 7a) and by the reorientation of brown biotite due to kinking and suggests that k_{max} delineates the zone axis for reoriented planar markers. Consequently, the magnetic lineation in the SE domain is the result of a composite magnetic fabric and indicates a partial structural and metamorphic overprint of the Murray pluton.

ORIGIN OF FABRICS IN THE MURRAY PLUTON

The rapid increase of metamorphic grade across the Murray pluton from greenschist facies in the SE domain to amphibolite facies accompanied by incipient melting of felsic minerals near the contact with the SIC requires a

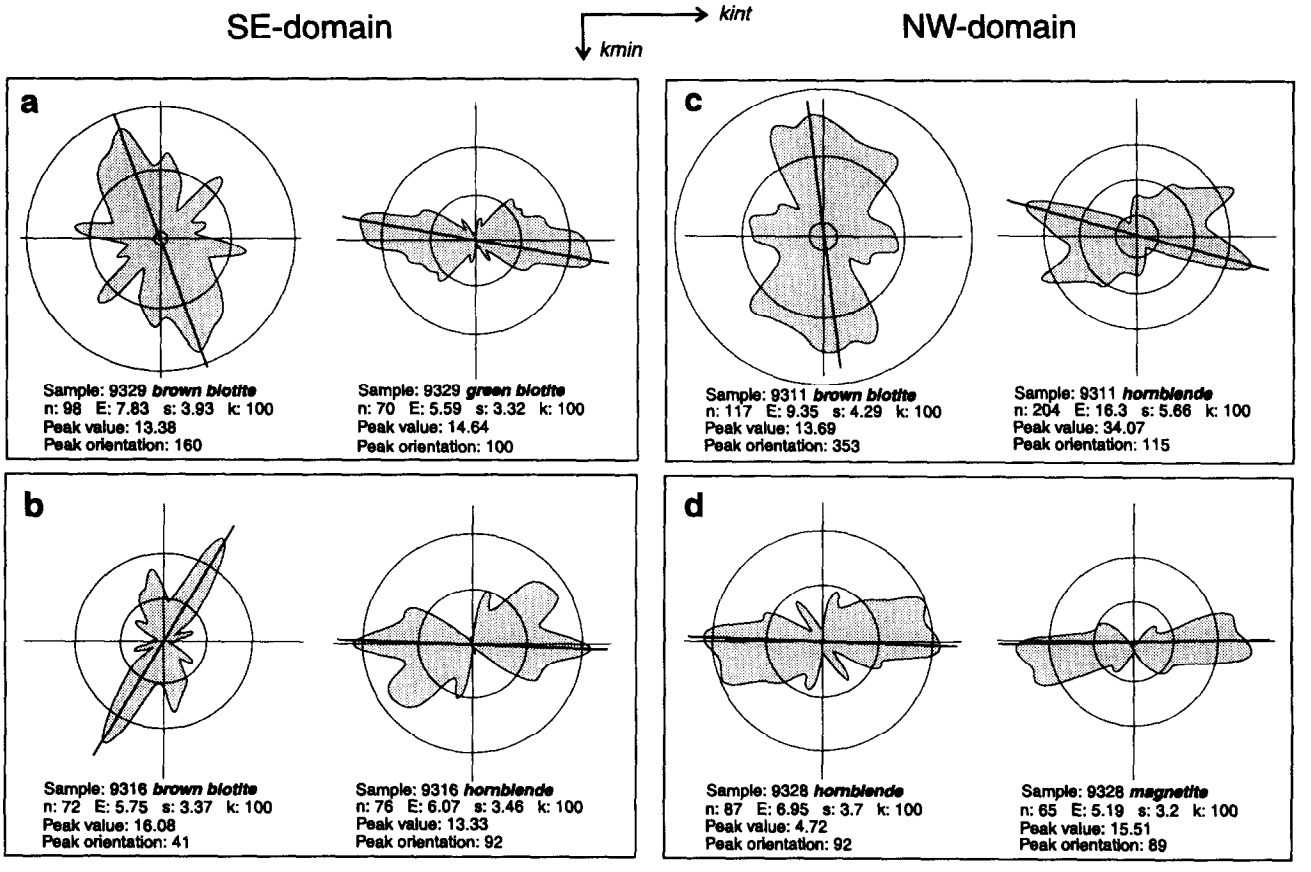

Fig. 8. Frequency rose diagrams for the azimuth of mineral outlines of igneous (biotite) and metamorphic (green biotite, hornblende and magnetite) minerals perpendicular to magnetic lineation. The largest circle is at 1.8σ above random distribution E, the smallest one represents the frequency for E. Therefore, peaks above this circle are statistically significant.

substantial heat source north of the pluton. This cannot be explained by a regional geothermal gradient, and must be a local effect. The adjacent norite of the SIC (Fig. 2) which was emplaced 530 Ma later than the Murray pluton is the natural candidate for the heat source. The increase in grain size towards the northwest, and dynamic recrystallization together with annealing and recovery features in quartz in the NW domain indicate that fabric formation was coeval with contact metamorphism of the Murray pluton. The observed concentration of solid state strain in the NW domain and the northwestward increase in shape fabric and magnetic fabric anisotropy is also consistent with this interpretation.

Two lines of evidence from the magnetic fabric study indicate a gradient in the structural overprint. (1) Magnetic anisotropy magnitude in the NW domain increases up to a maximum at the contact with the SIC, where the magnetic fabric correlates with the petrofabric visible in outcrop and thin section (Fig. 6c). Near the SE margin, granites are not affected by any metamorphic recrystallization and have a magnetic foliation that is close to the foliation identified in the field (samples MP1, MP24, 9331, Fig. 5a). The structural overprint recorded by the magnetic fabric is therefore present only within a 1.8 km wide zone parallel to the contact with the SIC. (2) The tendency for an increase in degree of anisotropy with increasing oblateness of the susceptibility ellipsoid (Fig. 6a) has been observed in previous magnetic fabric studies of granitoids (e.g. Archanjo *et al.* 1994, 1995, Leblanc *et al.* 1994). This may be related to both the strain path in the rock and strain intensity, such as along the contacts with the country rocks.

The limited extent of contact-parallel overprint in the Murray pluton and its decrease in intensity toward the SE, suggests that development of this foliation was facilitated by the strong thermal gradient set up in the pluton due to heat transfer from the SIC. The lack of a metamorphic foliation in mafic metavolcanics within the thermal aureole of the SIC at both extremities of the Murray pluton suggests that foliation development in the footwall granitoids is a local structural phenomenon that may be attributed to deformation related to emplacement of the SIC.

The magnetic fabric data and microstructure suggest that the origin of the structural domains can be best explained as a result of the non-coaxial superposition of two separate deformation pulses. However, approaching the northwestern contact of the pluton, NW plunging magnetic lineations change progressively to SW plunges, parallel to the strike of the higher strained fabrics. Magnetic lineation plunges, which are moderate at the transition between the two domains, are steepest where strains are highest (Fig. 5b). Therefore, a minor component of compression leading to subvertical escape of material close to the contact with the SIC may have accompanied the fabric overprint in the Murray pluton.

IMPLICATIONS FOR THE STRUCTURAL EVOLUTION OF THE SUDBURY BASIN

The origin of the Sudbury Igneous Complex (SIC) and nature of its elliptical map pattern (Fig. 1) and asymmetric deep structure are controversial. Recently, workers have proposed that the Sudbury Basin is a synform and that the SIC originated as a flat horizontal impact melt sheet prior to shortening by folding and/or NW thrusting along the South Range Shear Zone (Shanks & Schwerdtner 1991, Milkereit *et al.* 1992, Cowan & Schwerdtner 1994). This contrasts with earlier hypotheses in which the funnel-shape geometry of the SIC is primary in origin (Muir 1984, Naldrett 1984). The geometric continuity of foliation trajectories, at least across the SE margin of the Murray pluton (Fig. 2) and the strain fabric observed in the Huronian footwall beyond the metamorphic aureole of the norite of the SIC suggests that ductile deformation preceded the emplacement of the norite.

Northward bulk translation of the Huronian footwall rocks on south dipping thrust surfaces of the South Range Shear Zone possibly accommodated by fault block imbrication may have contributed to the shortening of the SIC and to the NW–SE asymmetry of the Sudbury Basin. Translation also explains the widespread lack of ductile deformation in the South Range norite and Huronian footwall aureolè. However, translation cannot account for the observed strain gradient in the NW domain of the Murray pluton. During buckling of the SIC and its enveloping rocks, strains will have been concentrated preferentially in the low competency layers (Ramberg 1963). The thermally softened NW part of the Murray pluton was a favorable location for the accumulation of such contact strain.

Mineralogical and microstructural evidence indicates that contact strain in the NW domain of the Murray pluton was acquired during emplacement of the norite. However, isotropic fabrics in the norite and contact metamorphic mafic Huronian volcanics as well as recovery and annealing of quartz in the NW domain suggest that emplacement and cooling of the norite outlasted deformation of the SIC and enveloping rocks. These relationships suggest that emplacement of the norite occurred during and/or after the buckle folding of the SIC, which points to an intrusive origin of the norite (see also Chai & Eckstrand 1993).

CONCLUSIONS

Field measurements, microstructural observations and magnetic fabric analysis show that the Murray pluton is divisible into two distinct structural and metamorphic domains. AMS analysis provides clear evidence that a contact metamorphic fabric, related to emplacement of the norite, overprints an earlier fabric in the granitoids. The strength of this overprint increases gradually towards the contact with the norite. In the SE domain, in places where both fabrics have similar intensities, the magnetic lineation is parallel to the intersection lineation indicating a composite magnetic fabric. These results suggest that (1) a regional, pre-SIC deformation occurred in the Huronian footwall, (2) local deformation in the Murray pluton resulted from NW–SE shortening accommodated by buckle folding during emplacement and cooling of the norite, and (3) the norite is intrusive in origin rather than part of an impact melt. The metamorphic gradient documented in the Murray pluton had a profound influence on magnetic susceptibilities and fabrics of the metagranitoids.

Acknowledgements—This work was funded by NSERC and AG LITHOPROBE. We thank E. J. Cowan, J. Dehls, B. O. Dressler, J. J. Fawcett, W. Klemens, W. Meyer, L. Pryer and R. Vernon for many helpful discussions and J. S. Brett for assistance in the field. B. A. van der Pluijm and J. L. Bouchez reviewed the manuscript for the journal, and we are grateful for their constructive criticism. U.R. gratefully acknowledges funding by the Deutscher Akademischer Austauschdienst (scholarship HSPII-AUFE). LITHOPROBE publication number 758.

REFERENCES

Archanjo, C. J., Bouchez, J. L., Corsini, M. & Vauchez, A. 1994. The Pombal granite pluton: magnetic fabric, emplacement and relationships with the Brasiliano strike-slip setting of NE Brazil (Paraiba State). *J. Struct. Geol.* **16**, 323–335.

Archanjo, C. J., Launeau, P. & Bouchez, J. L. 1995. Magnetic fabric vs. magnetite and biotite shape fabrics of the magnetite-bearing granite pluton of Gameleiras (Northeast Brazil). *Phys. Earth Planet. Interiors* **89**, 63–75.

Benn, K., Rochette, P., Bouchez, J. L. & Hattori, K. 1993. Magnetic susceptibility, magnetic mineralogy and magnetic fabrics in a late Archean granitoid–gneiss belt. *Precambrian Res.* **63**, 59–81.

Borradaile, G. 1987. Anisotropy of magnetic susceptibility: rock composition versus strain. *Tectonophysics* **138**, 327–329.

Borradaile, G. 1991. Correlation of strain with anisotropy of magnetic susceptibility (AMS). *Pure & Appl. Geophys.* **135**, 17–29.

Borradaile, G. & Tarling, D. H. 1981. The influence of deformation mechanisms on magnetic fabrics in weakly deformed rocks. *Tectonophysics* **77**, 151–168.

Bouchez, J. L. & Gleizes, G. 1995. Two-stage deformation of the Mont-Louis-Andorra granite pluton (Variscan Pyrenees) inferred from magnetic susceptibility anisotropy. *J. geol. Soc. Lond.* **152**, 669–679.

Bouchez, J. L., Gleizes, G., Djouadi, T. & Rochette, P. 1990. Microstructure and magnetic susceptibility applied to the emplacement kinematics of granites: the example of the Foix pluton (French Pyrenees). *Tectonophysics* **184**, 157–171.

Card, K. D. 1978. Metamorphism of Middle Precambrian (Aphebian) rocks of the Eastern Southern Province. In: Metamorphism in the Canadian Shield. *Geol. Surv. pap. Can.* **78-10**, 269–282.

Card, K. D., Church, W. R., Franklin, J. M., Robertson, J. A., West, G. F. & Young, G. M. 1972. The Southern Province. In: *Variations in Tectonic Style in Canada* (edited by Price, R. A. and Douglas, R. J. W.). *Geol. Assoc. Can. Spec. Paper* **11**, 335–380.

Chai, G. & Eckstrand, O. R. 1993. Origin of the Sudbury Igneous Complex, Ontario — differentiate of two separate magmas. In: Current Research, Part E, *Geol. Surv. pap. Can.* **93-1E**, 219–230.

Corfu, F. & Andrews, A. J. 1986. A U–Pb for mineralized Nipissing Diabase, Gowganda, Ontario. *Can. J. Earth Sci.* **23**, 107–109.

Cowan, E. J. & Schwerdtner, W. M. 1994. Fold origin of the Sudbury Basin. In: *Proceedings of the Sudbury–Noril'sk Symposium* (edited by Lightfoot, P. C. & Naldrett, A. J.). *Ontario Geological Survey Special Volume* **5**, 45–56.

Cruden, A. R. & Launeau, P. 1994. Structure, magnetic fabric and emplacement of the Archean Lebel Stock, SW Abitibi Greenstone Belt. *J. Struct. Geol.* **16**, 677–691.

Dietz, R. S. 1964. Sudbury structure as an astrobleme. *J. Geol.* **72**, 412–434.

Dressler, B. O., Gupta, V. K. & Muir, T. L. 1991. The Sudbury Structure. In: *Geology of Ontario* (edited by Thurston, P. C.,

Williams, H. R., Sutcliffe, R. H. & Stott, G. M.). *Ontario Geological Survey Special* Volume **4**, 593–626.

Flinn, D. 1962. On folding during three dimensional progressive deformation. *Q. Jl geol. Soc. Lond.* **118**, 385–428.

Frarey, M. J., Loveridge, W. D. & Sullivan, R. W. 1982. A U–Pb zircon age for the Creighton granite, Ontario. In: *Rb–Sr and U–Pb Isotopic Age Studies*, Report **5**. *Geol. Surv. pap. Can.* **81-1C**, 129–132.

Grégoire, V., de Saint Blanquat, M., Nedelec, A. & Bouchez, J. L. 1996. Shape anisotropy versus magnetic interactions of magnetic grains: experiments and application to AMS in granitic rocks. *Geophys. Res. Lett.* **22**, 2765–2768.

Grieve, R. A. F., Stöffler, D. & Deutsch, A. 1991. The Sudbury Structure: controversial or misunderstood? *J. geophys. Res.* **96**, 22753–22764.

Hargraves, R. B., Johnson, D. & Chan, C. Y. 1991. Distribution anisotropy: the cause of AMS in igneous rocks? *Geophys. Res. Lett.* **18**, 2193–2196.

Hext, G. R. 1963. The estimation of second-order tensors, with related tests and design. *Biometrika* **50**, 353–373.

Hibbard, M. J. 1987. Deformation of incompletely crystallized magma systems: granite gneisses and their tectonic implications. *J. Geol.* **95**, 543–561.

Housen, B. A., Richter, C. & van der Pluijm, B. A. 1993. Composite magnetic anisotropy fabrics: experiments, numerical models, and implications for the quantification of rock fabrics. *Tectonophysics* **220**, 1–12.

Housen, B. A., van der Pluijm, B. A. & Essene, E. J. 1995. Plastic behavior of magnetite and high strains obtained from magnetic fabrics in the Parry Sound shear zone, Ontario Grenville Province. *J. Struct. Geol.* **17**, 265–278.

Jelinek, V. 1978. Statistical processing of anisotropy of magnetic susceptibility measured on groups of specimens. *Stud. Geophys. Geodyn.* **22**, 50–62.

Jelinek, V. 1981. Characterization of the magnetic fabrics of rocks. *Tectonophysics* **79**, T63–T67.

Kerrich, R., Allison, I., Barnett, R. L., Moss, S. & Starkey, J. 1980. Microstructural and chemical transformations accompanying deformation of granite in a shear zone at Mieville, Switzerland; with implications for stress corrosion cracking and superplastic flow. *Contr. Miner. Petrol.* **73**, 221–242.

Krogh, T. E. & Davis, G. L. 1969. Old isotopic ages in the northwestern Grenville Province, Ontario. *Geol. Assoc. Canada Spec. Paper* **5**, 189–192.

Krogh, T. E., Davis, D. W. & Corfu, F. 1984. Precise U–Pb zircon and baddeleyite ages for the Sudbury area. In: *The Geology and Ore Deposits of the Sudbury Structure* (edited by Pye, E. G., Naldrett, A. J. & Giblin, P. E.). Ontario Geological Survey Special Volume 1, 97–136.

Leblanc, D., Gleizes, G., Lespinasse, P., Olivier, Ph. & Bouchez, J. L. 1994. The Maladeta granite polydiapir, Spanish Pyrenees: a detailed magneto-structural study. *J. Struct. Geol.* **16**, 223–235.

Lienert, B. R. 1991. Monte Carlo simulation of errors in the anisotropy of magnetic susceptibility: a second-rank symmetric tensor. *J. geophys. Res.* **96**, 19,539–19,544.

Milkereit, B., Green, A. & Sudbury Working Group. 1992. Deep geometry of the Sudbury structure from seismic reflection profiling. *Geology* **20**, 807–811.

Muir, T. L. 1984. The Sudbury Structure; considerations and models for an endogenic origin. In: *The Geology and Ore Deposits of the Sudbury Structure* (edited by Pye, E. G., Naldrett, A. J. & Giblin, P. E.). Ontario Geological Survey Special Volume 1, 449–490.

Muir, T. L. & Peredery, W. V. 1984. The Onaping Formation. In: *The Geology and Ore Deposits of the Sudbury Structure* (edited by Pye, E. G., Naldrett, A. J. & Giblin, P. E.). Ontario Geological Survey Special Volume 1, 139–210.

Naldrett, A. J. 1984. Summary, discussion, and synthesis. In: *The Geology and Ore Deposits of the Sudbury Structure* (edited by Pye, E. G., Naldrett, A. J. & Giblin, P. E.). Ontario Geological Survey Special Volume 1, 533–570.

Nye, J. F. 1957. *Physical Properties of Crystals*. Oxford Scientific Publications, 329 pp.

Pye, E. G., Naldrett, A. J. & Giblin, P. E. 1984. The geology and ore deposits of the Sudbury Structure. Ontario Geological Survey Special Volume 1.

Ramberg, H. 1963. Strain distribution and geometry of folds. *Bull. geol. Instn. Univ. Upsala* **42**, 1–20.

Richter, C., Ratschbacher, L. & Frisch, W. 1993. Magnetic fabrics, crystallographic preferred orientation, and strain of progressively metamorphosed pelites in the Helvetic Zone of the Central Alps (Quartenschiefer Formation). *J. geophys. Res.* **98**, 9557–9570.

Riller, U., Cruden, A. R. & Schwerdtner, W. M. 1994. Microstructural and magnetic fabric analysis of the Murray Pluton, Eastern Penokean Orogen. *Geol. Soc. Am. Abstr. Progr.* **26**, 7.

Rochette, P. 1987. Magnetic susceptibility of the rock matrix related to magnetic fabric studies. *J. Struct. Geol.* **9**, 1015–1020.

Rochette, P. & Vialon, P. 1984. Development of planar and linear fabrics in Dauphinois shales and slates (French Alps) studied by magnetic anisotropy and its mineralogical control. *J. Struct. Geol.* **6**, 33–38.

Rochette, P., Jackson, M. & Aubourg, C. 1992. Rock magnetism and the interpretation of anisotropy of magnetic susceptibility. *Rev. Geophys.* **30**, 209–226.

Schwerdtner, W. M., Morgan, J. & Stott, G. M. 1985. Contacts between greenstone belts and gneiss complexes within the Wabigoon Subprovince, Northwestern Ontario. In: *Evolution of Archean Supracrustal Sequences* (edited by Ayres, L. D., Thurston, P. C., Card, K. D. & Weber, W.). *Geol. Assoc. Can. Spec. Paper* **28**, 117–123.

Shanks, W. S. & Schwerdtner, W. M. 1991. Structural analysis of the central and southwestern Sudbury structure, Southern Province, Canadian Shield. *Can. J. Earth Sci.* **28**, 411–430.

Stephenson, A. 1994. Distribution anisotropy: two simple models for magnetic lineation and foliation. *Phys. Earth Planet. Interiors* **82**, 49–53.

Stockwell, C. H. 1982. Proposals for the time classification and correlation of Precambrian rocks and events in Canada and adjacent areas of the Canadian Shield. *Geol. Surv. pap. Can.* **80-19**, 135P.

Tarling, D. H. & Hrouda, F. 1993. *The Magnetic Anisotropy of Rocks*. Chapman and Hall.

Thurston, P. C. 1991. Proterozoic Geology of Ontario: Introduction. In: *Geology of Ontario* (edited by Thurston, P. C., Williams, H. R., Sutcliffe, R. H. & Stott, G. M.). Ontario Geological Survey Special Volume 4, Part 2, 543–548.

Tullis, J. 1983. Deformation of feldspars. In: *Feldspar Mineralogy* (2nd edn) (edited by Ribbe, P. H.). *Miner. Soc. Am. Rev. Mineral.* **2**, 297–323.

Van der Molen, I. & Paterson, M. S. 1979. Experimental deformation of partially melted granite. *Contr. Miner. Petrol.* **70**, 299–318.

Van Schmus, W. R. 1976. Early & middle Proterozoic history of the Great Lakes area, North America. *Phil. Trans. R. Soc. Lond.* **280**, 606–628.

Vernon, R., Williams, V. A. & D'Arcy, W. F. 1983. Grain-size reduction and foliation development in a deformed granitoid batholith. *Tectonophysics* **92**, 123–145.

Voll, G. 1980. Ein Querprofil durch die Schweitzer Alpen vom Vierwaldstätter See zur Wurzelzone—Strukturen und ihre Entwicklung durch Deformationsmechanismen wichtiger Minerale. *Neues. Jahrb. Geol. Paläontol. Abh.* **160**, 321–335.

Wetherill, G. W., Davis, G. L. & Tilton, G. R. 1960. Age measurements on minerals from the Cutler batholith, Cutler, Ontario. *J. geophys. Res.* **65**, 2461–2466.

Winkler, H. G. F. 1979. *Petrogenesis of Metamorphic Rocks*. Springer Verlag.